ELSEVIER

Journal of Crystal Growth 160 (1996) 310–319

JOURNAL OF CRYSTAL GROWTH

Controlling the group II composition in CdZnTe alloys grown by organometallic vapor phase epitaxy: a kinetic model

Menno J. Kappers, Anthony H. McDaniel, Robert F. Hicks *

Department of Chemical Engineering, University of California at Los Angeles, Los Angeles, California 90024-1592, USA

Received 7 July 1995; accepted 17 October 1995

Abstract

The organometallic vapor phase epitaxy (OMVPE) of CdTe and ZnTe has been examined in a hot-wall, laminar-flow reactor. It was found that cadmium and zinc are produced in excess on the film surface during OMVPE. The excess group II elements sublime off the surface and are deposited downstream on the cold reactor walls. Based on these and other results, a kinetic model has been derived for CdZnTe OMVPE. The elementary reactions included in this model are the adsorption of the organometallic precursors, the desorption of the alkyl ligands, film growth, and the desorption of Zn and Cd metal. The predictions of the model have been compared to the Zn segregation data reported in the literature. This analysis reveals that the distribution of the group II elements between phases is relatively insensitive to the process conditions, i.e. temperature and VI/II ratio. However, it is strongly influenced by the intrinsic kinetic parameters, i.e. the difference in the Zn and Cd sublimation energies and the relative sticking probabilities of the organometallic precursors.

1. Introduction

The growth of II–VI semiconductor alloy films on Si(001), GaAs(001) or Al_2O_3(0001) substrates is an important step in the manufacture of large-area infrared focal-plane arrays (IRFPAs) [1–7]. Epitaxial CdZnTe films have been deposited on a number of different substrates by liquid-phase epitaxy (LPE) [8,9], molecular beam epitaxy (MBE) [10–14] and organometallic vapor phase epitaxy (OMVPE) [15–18]. The latter technique has been shown to be successful for the reproducible growth of high-quality layers [17,18]. Thin films of CdZnTe grown by OMVPE are used as buffer layers prior to the growth of HgCdTe photodiodes. Widely used are infrared detectors with a spectral cut-off at 10 μm, consisting of $Hg_{1-x}Cd_xTe$ with $x = 0.215$. Because the quality of the HgCdTe is strongly affected by lattice mismatch with the underlying substrate, the zinc mole fraction in the CdZnTe film must be held at $4.0 \pm 0.1\%$. Therefore, composition control is a critical issue in growing CdZnTe alloys by OMVPE.

The composition diagram for the solid versus the vapor in the OMVPE of CdZnTe was determined experimentally at 714 K by Ahlgren et al. [16]. It was reported that the incorporation of zinc is strongly favored over cadmium. The steepness of the composition diagram at low Zn mole fractions makes it difficult to achieve the desired alloy composition uniformly throughout the CdZnTe buffer layer. A thermodynamic equilibrium analysis failed to explain the segregation behaviour of the group II elements.

We and other researchers have found that surface

* Corresponding author.

SSDI 0022-0248(95)00935-3

reactions play an important role during the OMVPE of II–VI compound semiconductors [19–27]. The observed activation energies for film growth below 673 K are between 25 and 30 kcal/mol, which are less than half the energies required to pyrolyze the organometallic molecules in the gas [28–30]. The decompositions rates of the organotelluride compounds are greatly accelerated when the reaction is carried out in the presence of a growing CdTe film [21,22]. Moreover, the hydrocarbon products formed during OMVPE, and their dependence on the growth conditions, can only be explained by surface reactions of the adsorbed alkyl ligands [24].

The composition of CdZnTe thin films is also determined by surface reactions during growth. Under steady-state deposition conditions, the Zn mole fraction in the bulk must equal the Zn coverage on the surface. The Zn coverage is in turn governed by the relative rates of adsorption and desorption of the species containing zinc and cadmium. In this paper, we identify the elementary surface processes that are involved in the growth of CdZnTe by OMVPE. A kinetic model is derived from this information, and the predictions of the model are compared to the Zn segregation data obtained by Ahlgren et al. [16]. The analysis reveals that the group II composition in the solid versus the vapor is very sensitive to the intrinsic kinetics, but is relatively insensitive to the process conditions (temperature and VI/II ratio). Below we discuss the implications of these findings with regard to controlling the Zn concentration in OMVPE-grown CdZnTe.

2. Experimental methods

Deposition of polycrystalline CdTe was carried out in an atmospheric-pressure, horizontal-flow reactor [24]. The reactor consisted of a glass tube, 20 cm long, with a heated section in the middle of the tube, 5 cm long by 0.2 cm in diameter. The reaction temperature was maintained to within 2 K over 3 cm of the heated zone by a resistively heated, stainless-steel block that surrounded the glass tube. Heat exchangers were mounted on both sides of the stainless-steel block, and they quickly cooled the glass down to 300 K. Electronic-grade dimethylcadmium (DMCd), diethylzinc (DEZn), dimethyltelluride (DMTe) and diisopropyltelluride (DIPTe) were contained in stainless-steel bubblers submerged in thermostatic baths. The organometallic precursors were vaporized into a flow of helium, then diluted to 200 ml/min with hydrogen and fed to the reactor. The H_2 and He (99.995%) were purified by passing them through deoxygenation traps and 13X molecular sieves held at 195 K. Prior to each experiment, a passivating layer of CdTe or ZnTe was deposited at 653 K in hydrogen on the clean glass tube. The OMVPE reactions were carried out at 106 cm/s inlet gas velocity (STP), 1 atm total pressure, 653–673 K, $(1–30)\times 10^{-4}$ atm of DMCd, DEZn and DMTe or DIPTe, and H_2 carrier gas.

The OMVPE reactor was interfaced to an HP 5890A gas chromatograph, equipped with a Restek Rt_x-1 megabore capillary column, 30 m long, and a flame-ionization detector. The reactor inlet and outlet streams were directly injected onto the column. The consumption rates of the organometallic compounds were determined from the changes in the integrated GC signals from the inlet to the outlet of the reactor. These consumption rates agreed to within 10% of the mass of the film deposited as measured by the increase in weight of the tube. After growth, the films deposited in the tubes were analysed by X-ray diffraction.

3. Experimental results

The decomposition rate of the organometallic precursors varies with the partial pressure of the sources. Fig. 1 shows the dependence of the DMCd and DMTe consumption rates on their partial pressures during CdTe film growth at 653 K. The consumption rate of DMCd increases three times as its amount in the feed increases from 8.0×10^{-5} to 2.0×10^{-3} atm. At the same time, the decomposition rate of DMTe is unchanged. On the other hand, as the partial pressure of DMTe increases from 8.0×10^{-5} to 2.0×10^{-3} atm, its consumption rate increases three times, while the consumption rate of DMCd remains constant. Regardless of which precursor partial pressure is changed, the curves show that whenever the VI/II ratio falls below 2, the DMCd is consumed faster than the DMTe.

In order to determine what happens to the excess

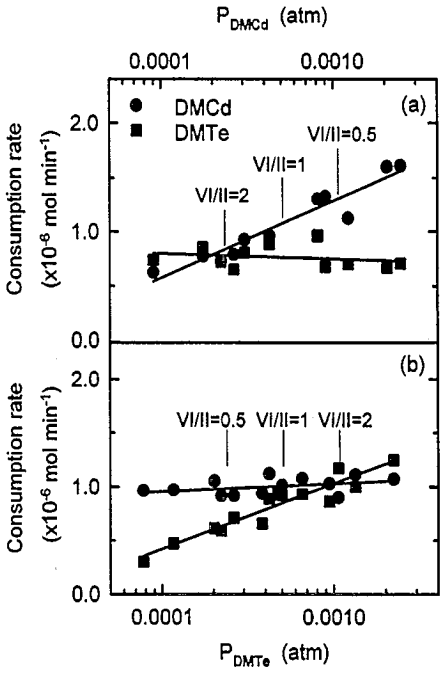

Fig. 1. The dependence of the DMCd and DMTe consumption rates on their inlet partial pressures. (a) Varying the DMCd partial pressure at 5.5×10^{-4} atm DMTe. (b) Varying the DMTe partial pressure at 5.0×10^{-4} atm DMCd (0.85 atm H_2 and 653 K).

cadmium produced in the OMVPE reactor, the films deposited on the glass have been analyzed by X-ray diffraction after the experiment. Inside the heated region, polycrystalline cadmium telluride is deposited as evidenced by three sharp peaks at 2θ equal to 23.7, 39.2 and 46.4°. Whereas just downstream of the hot zone, cadmium metal is deposited, yielding diffraction peaks at 2θ equal to 31.6, 34.5 and 38.1°. These data reveal that the excess cadmium, liberated from the heterogeneous decomposition of DMCd, sublimes off the film surface and is transported out of the reactor where it plates out on the cold walls of the tube.

The same experiment has been performed for ZnTe OMVPE using DEZn and DIPTe, and analogous results were obtained. The reaction was carried out at 673 K, 5.0×10^{-4} atm DIPTe, and a VI/II ratio of 1.0. Inside the hot tube, ZnTe is deposited preferentially in the (111) orientation, yielding a single sharp peak at 2θ equal to 25.2°. By contrast, downstream of the reactor three peaks at 36.1, 38.9 and 43.1° are recorded that are characteristic of zinc metal. In conclusion, sublimation of the group II elements occurs during the OMVPE of II–VI materials. We anticipate that this process should have a major impact on the composition of II–VI alloy films.

4. Kinetic model

Based on our previous work [24,25] and the results presented above, a heterogeneous reaction mechanism may be proposed for CdZnTe OMVPE. This mechanism is presented in Table 1.

The organometallic precursors adsorb onto empty surface sites, represented as "$*$" in Reactions (1)–(3). Once adsorbed, they dissociate via the transfer of the alkyl groups to adjacent sites, Steps (4) to (6). The ZnR$*$, CdR$*$ and TeR$*$ species formed after breaking the first alkyl-metal bonds are distinguishable from R$*$ species in that the former alkyls are bonded to adsorbed metal atoms, whereas the latter alkyls are bonded to atoms that are part of the crystal. The adsorbed metal atoms become part of the crystal surface in the film growth Reactions (11) and (12). However before this can occur, the alkyl

Table 1
Surface reaction mechanism for CdZnTe film growth by OMVPE

	Reaction	Number
Adsorption	DEZn$+*\rightarrow$DEZn$*$	(1)
	DMCd$+*\rightarrow$DMCd$*$	(2)
	DETe$+*\rightarrow$DETe$*$	(3)
Dissociation	DEZn$*+*\rightarrow$RZn$*+$R$*$	(4)
	DMCd$*+*\rightarrow$RCd$*+$R$*$	(5)
	DETe$*+*\rightarrow$RTe$*+$R$*$	(6)
Alkyl desorption	RZn$*\rightarrow$R$\cdot+$Zn$*$	(7)
	RCd$*\rightarrow$R$\cdot+$Cd$*$	(8)
	RTe$*\rightarrow$R$\cdot+$Te$*$	(9)
	R$*\rightarrow$R$\cdot+*$	(10)
Film growth	Zn$*+$Te$*\rightarrow$$ZnTe_b+2*$	(11)
	Cd$*+$Te$*\rightarrow$$CdTe_b+2*$	(12)
Metal desorption	Cd$*\rightarrow$Cd$+*$	(13)
	Zn$*\rightarrow$Zn$+*$	(14)

Here $*$ = (empty) surface site; R = CH_3 or C_2H_5; $\cdot$ = radical; b = bulk.

groups must desorb off the surface. In our model, alkyl desorption is represented as a first-order process in which hydrocarbon radicals are released into the gas, Steps (7)–(10). Desorption of the alkyl groups from Zn and Cd sites is assumed to occur faster than that from Te sites. In other words, breaking the second alkyl-tellurium bond, Reaction (9), is the rate-limiting step in film growth [23,24]. The faster rate of alkyl desorption from Zn and Cd causes these elements to be in excess on the surface. The excess group II elements desorb as shown in Reactions (13) and (14).

Recently, we identified the hydrocarbons produced from CdTe OMVPE with dimethylcadmium, dimethyltelluride, and diisopropyltelluride [24]. The different types of hydrocarbons formed, and their dependence on the hydrogen pressure in the reactor, led us to conclude that the alkyl groups undergo several reactions on the film surface, including radical desorption, recombination, hydrogenation and disproportionation. Nevertheless, in all cases the rate-limiting process appeared to be the breaking of the second Te-alkyl bond. This was consistent with the observation that the apparent activation energy for film growth was independent of the Te source used and the H_2 pressure. Therefore, for the purpose of predicting the film growth rate and composition it is not necessary to account for all the pathways by which hydrocarbons are formed in this reaction. Instead these reactions may be lumped into a single alkyl-radical desorption step as is done in Table 1.

During the OMVPE of $Cd_{1-y}Zn_yTe$, the mole fraction of zinc (y) and cadmium ($1-y$) in the film is equal to the mole fraction of these species on the surface of the film:

$$y = \frac{\theta_{Zn}}{\theta_{Zn} + \theta_{Cd}}, \tag{15}$$

$$1 - y = \frac{\theta_{Cd}}{\theta_{Zn} + \theta_{Cd}}. \tag{16}$$

Here, θ_{Zn} and θ_{Cd} are the fractional coverages of Zn and Cd on the surface. Under steady-state growth conditions, these coverages are constant. Their values are determined by the relative rates of adsorption of the organometallic molecules, desorption of the alkyl groups, and desorption of Zn and Cd metal.

The adsorption rates of the organometallic molecules are assumed to be given by [24]:

$$r_{a,OM} = \tfrac{1}{4}\bar{v}_{OM} S_{OM} C_{OM} \theta_v, \tag{17}$$

where $\bar{v}_{OM}$, S_{OM} and C_{OM} are the mean molecular speed (cm/s), the initial sticking probability and the concentration of the organometallic molecules (mol/cm^3), and θ_v is the fraction of vacant adsorption sites. The sticking coefficient of the different molecules is believed to vary from 1×10^{-5} to 1×10^{-3} [20,24,31].

No distinction is made for the desorption of the alkyl groups from adsorbed Zn and Cd atoms, or from the crystal surface (*) (Reactions (7), (8) and (10)). These are assumed to be first-order reactions with the same activation energy:

$$r_{d,ZnR} = \frac{n}{N} A_d e^{(-E_d/RT)} \theta_{ZnR}, \tag{18}$$

$$r_{d,CdR} = \frac{n}{N} A_d e^{(-E_d/RT)} \theta_{CdR}, \tag{19}$$

$$r_{d,R} = \frac{n}{N} A_d e^{(-E_d/RT)} \theta_R, \tag{20}$$

where n is the number of adsorption sites per unit area of surface (cm^{-2}), N is Avogadro's number, and A_d and E_d are the frequency factor (s^{-1}) and the activation energy (kcal/mol) for the desorption of the alkyl radicals. The number of adsorption sites is set equal to 2 per (6.29 Å)^2, where 6.29 Å is the average lattice constant for CdZnTe. The pre-exponential factor, A_d, and the activation energy, E_d, are assumed to equal 1×10^{13} s^{-1} and 32 kcal/mol, respectively [20,23]. The desorption energies of R from Cd and Zn sites are assumed equal in order to avoid unnecessary complexity in the model. Equal values are also justified given that the average bond dissociation energies of DMCd and DEZn are the same [32].

Below 673 K, the rate-limiting step in film growth is the breaking of the second alkyl-Te bond (Reaction (9)) [24]. This process is also assumed to be first-order in the adsorbed species:

$$r_{d,TeR} = r_g = \frac{n}{N} A_g e^{(-E_g/RT)} \theta_{TeR}, \tag{21}$$

where A_g and E_g are the frequency factor (s^{-1}) and the activation energy (kcal/mol) for this reaction. In general, E_g is greater than E_d.

The sublimation of Zn and Cd from the crystal surface is represented by the following equations:

$$r_{d,Zn} = \frac{n}{N} A_d e^{(-\Delta H_{sub}^{Zn}/RT)} \theta_{Zn}, \quad (22)$$

$$r_{d,Cd} = \frac{n}{N} A_d e^{(-\Delta H_{sub}^{Cd}/RT)} \theta_{Cd}. \quad (23)$$

Here ΔH_{sub}^{Zn} and ΔH_{sub}^{Cd} are the heats of sublimation of the metals, which are reported to be 29.5 and 25.9 kcal/mol [33]. Note that the value for Zn is the same within experimental error of the desorption energy of Zn from GaAs(100) [34,35]. All else being equal, a higher heat of sublimation for zinc relative to cadmium should yield $\theta_{Zn} > \theta_{Cd}$.

The steady-state coverages of the different alkyl species may be determined from their mass balances:

$$\frac{d\theta_{ZnR}}{dt} = r_{a,DEZn} - r_{d,ZnR} = 0, \quad (24)$$

$$\frac{d\theta_{CdR}}{dt} = r_{a,DMCd} - r_{d,CdR} = 0, \quad (25)$$

$$\frac{d\theta_{TeR}}{dt} = r_{a,DETe} - r_{d,TeR} = 0, \quad (26)$$

$$\frac{d\theta_{R}}{dt} = r_{a,DEZn} + r_{a,DMCd} + r_{a,DETe} - r_{d,R} = 0. \quad (27)$$

In these expressions, it is assumed that the hydrocarbon radicals do not readsorb onto the film after desorption. The steady-state coverage of Zn and Cd atoms may be determined from their mass-balances as well:

$$\frac{d\theta_{Zn}}{dt} = r_{d,ZnR} - y r_g - r_{d,Zn} = 0, \quad (28)$$

$$\frac{d\theta_{Cd}}{dt} = r_{d,CdR} - (1-y) r_g - r_{d,Cd} = 0. \quad (29)$$

The above equations can be solved when the following site balance is assumed:

$$\theta_{Zn} + \theta_{Cd} + \theta_{ZnR} + \theta_{CdR} + \theta_{TeR} + \theta_R + \theta_v = 1. \quad (30)$$

With seven unknown parameters and seven Eqs. (24)–(30), the coverages of Zn and Cd can be calculated for a given set of OMVPE reaction conditions. Then the alloy composition can be determined from the Zn and Cd coverages using Eqs. (15) and (16). However, since Eqs. (28) and (29) are implicit in θ_{Zn} and θ_{Cd}, the set of nine equations must be rearranged to yield a quadratic expression for the Zn mole fraction, y:

$$-K_{DETe}(K_{sub}-1)y^2 + [K_{DMCd} + K_{DEZn}K_{sub} + K_{DETe}(K_{sub}-1)]y - K_{DEZn}K_{sub} = 0, \quad (31)$$

where

$$K_{DEZn} = \bar{v}_{DEZn} S_{DEZn} x,$$

with

$$x = \frac{P_{DEZn}}{P_{DEZn} + P_{DMCd}},$$

$$K_{DMCd} = \bar{v}_{DMCd} S_{DMCd}(1-x),$$

$$K_{DETe} = \bar{v}_{DETe} S_{DETe}(VI/II),$$

with

$$VI/II = \frac{P_{DETe}}{P_{DEZn} + P_{DMCd}},$$

$$K_{sub} = e^{[(\Delta H_{sub}^{Zn} - \Delta H_{sub}^{Cd})/RT]}.$$

With the discriminant $b^2 - 4ac > 0$, the quadratic equation can be solved for the one solution of y which holds for $0 < y < 1$. From Eq. (31) it follows that:

$$y = \frac{K_{DMCd} + K_{DEZn}K_{sub} + K_{DETe}(K_{sub}-1)}{2K_{DETe}(K_{sub}-1)} + \left[\left(\frac{K_{DMCd} + K_{DEZn}K_{sub} + K_{DETe}(K_{sub}-1)}{2K_{DETe}(K_{sub}-1)} \right)^2 - \frac{K_{DEZn}K_{sub}}{K_{DETe}(K_{sub}-1)} \right]^{1/2}, \quad (32)$$

or

$$y = \frac{A + K_{sub} + B(K_{sub}-1)}{2B(K_{sub}-1)} + \left[\left(\frac{A + K_{sub} + B(K_{sub}-1)}{2B(K_{sub}-1)} \right)^2 - \frac{K_{sub}}{B(K_{sub}-1)} \right]^{1/2}, \quad (33)$$

where the constants A and B are defined as:

$$A = \frac{K_{DMCd}}{K_{DEZn}} = \left(\frac{M_{DEZn}}{M_{DMCd}}\right)^{1/2} \frac{S_{DMCd}}{S_{DEZn}} \frac{(1-x)}{x}, \tag{34}$$

and

$$B = \frac{K_{DETe}}{K_{DEZn}} = \left(\frac{M_{DEZn}}{M_{DETe}}\right)^{1/2} \frac{S_{DETe}}{S_{DEZn}} \frac{(VI/II)}{x}, \tag{35}$$

where M_{OM} is the molecular weight (g/mol) of the organometallic compound.

Inspection of Eqs. (31)–(35) reveals that the composition of the $Cd_{1-y}Zn_yTe$ film depends on three process variables: the mole fraction of zinc in the inlet gas (x), the VI/II ratio, and the substrate temperature. The film composition is also dependent on three kinetic parameters: the ratio of the sticking probabilities of DMCd over DEZn, the ratio of the sticking probabilities of DETe over DEZn, and the difference in the heats of sublimation of Zn and Cd. It follows then that the observed preference for zinc incorporation is due to the preferential adsorption of DEZn over DMCd, and/or to the higher heat of sublimation of Zn relative to that of Cd. Absent from Eq. (33) are the desorption energies of the alkyl groups from the Cd, Zn and Te sites. This means that the alloy composition is independent of the growth rate. The effect of the intrinsic kinetic parameters and the process variables on the composition of the alloy film is examined next.

5. Comparison of theory and experiment

Literature data on CdZnTe films grown over a broad range of alloy compositions are very limited [15,16]. However, valuable information can be obtained from a paper by Ahlgren et al. [16] in which OMVPE of CdZnTe on GaAs substrates is described for all alloy compositions, $0 \le y \le 1$. Deposition experiments were carried out using dimethylcadmium, diethylzinc and diethyltelluride in a horizontal, cold-wall reactor with the substrate temperature at 714 K, a VI/II ratio of one and a DETe partial pressure of about 3×10^{-4} atm at the reactor inlet. Strong temperature-dependent film growth was observed below 673 K, while the deposition rate remained constant in the temperature range between 673 and 714 K. It was suggested that the growth rate at high temperatures was limited by mass transport of the organometallic compounds to the substrate surface. In a number of studies it has been found that growth rates of thin semiconductor films remain constant or even decrease in the high temperature regime, and this has been ascribed to mass-transport limitations [16,19,32,36]. However, in a horizontal-flow reactor with an inlet pressure of the organometallic compounds above 1×10^{-4} atm, the growth rate in the mass-transport limit should exceed 20 μm/h [23,36]. In Ahlgren's study, the maximum growth rate achieved was 7 μm/h. Thus, the leveling off of the growth rate observed by these authors above 673 K is not due to mass-transport limitations. Instead it may be due to a low sticking probability of the organometallic compounds [20,26], or to the growth rate being limited by the feed rate of the organometallic compounds. We believe it is this latter case that applies to the experiments conducted by Ahlgren and coworkers. This conclusion is also consistent with the observation of a significant variation in growth rate and alloy film composition with position on the susceptor. Even though Ahlgren's data were taken under feed-rate-limited conditions, the adsorption rates of the organometallic compounds and the sublimation rates of Zn and Cd should still determine the film composition. Therefore, a meaningful comparison of our model to the data is possible, provided the average value of x in the reactor is compared to the average value of y in the film.

We have evaluated the parameters in Eq. (33) by fitting this function to the composition diagram of the solid versus the vapor as measured by Ahlgren et al. [16]. Shown in Fig. 2 is the effect of the relative sticking probabilities of DMCd and DEZn on the solid/vapor composition diagram. An excellent fit with Ahlgren's data is achieved for $S_{DMCd}/S_{DEZn} = 2.2$, $S_{DETe}/S_{DEZn} = 0.27$, and $\Delta H_{sub}^{Zn} - \Delta H_{sub}^{Cd} = 3.6$ kcal/mol. The adsorption rate of DEZn is enhanced with respect to that of DMCd by decreasing the S_{DMCd}/S_{DEZn} ratio. This results in a surface enrichment of zinc-containing species. The high sensitivity of the alloy composition to the S_{DMCd}/S_{DEZn} ratio illustrates that the composition is a strong function of

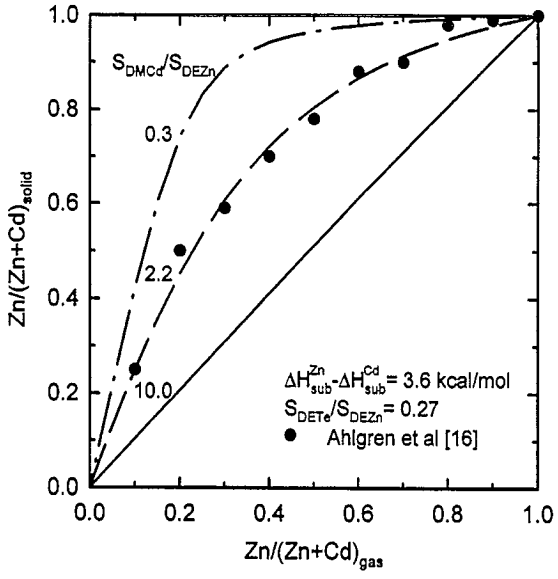

Fig. 2. The effect of varying the ratio of the sticking probability of DMCd over DEZn on the solid versus the vapor composition diagram for $Cd_{1-y}Zn_yTe$ OMVPE: (lines) kinetic model, and (●) experimental data.

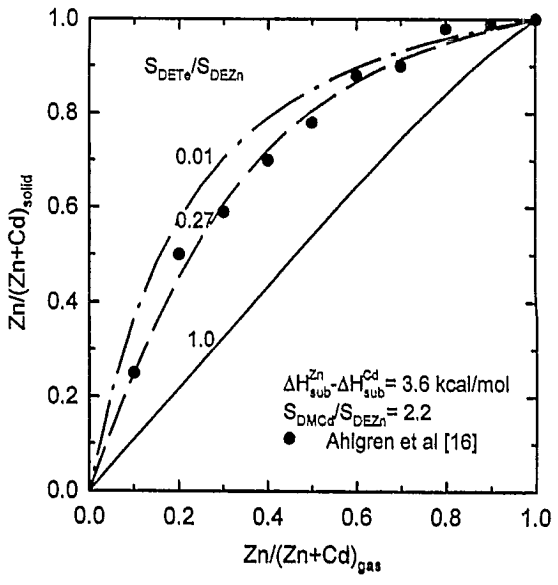

Fig. 3. The effect of varying the ratio of the sticking probability of DETe over DEZn on the solid versus the vapor composition diagram for $Cd_{1-y}Zn_yTe$ OMVPE: (lines) kinetic model, and (●) experimental data.

the relative adsorption rates of the group II organometallic compounds.

The sensitivity of y for the adsorption rate of DETe was investigated next. Shown in Fig. 3 is the effect of the relative sticking probabilities of DETe and DEZn on the solid/vapor composition diagram. This figure illustrates that Zn segregation only weakly depends on the DETe sticking coefficient upon decreasing S_{DETe}/S_{DEZn} from 0.27 to 0.01. However, the effect is significant for values above 0.3. This high sensitivity is unexpected since any change in S_{DETe} should change the surface coverage of Zn and Cd containing species equally. Apparently, the relatively high sticking coefficient of DMCd compensates for the higher heat of sublimation of zinc as the ratio S_{DETe}/S_{DEZn} approaches unity. In other words, the higher desorption rate of cadmium is counterbalanced by the higher adsorption rate of DMCd, when the rate of adsorption of DEZn equals that of DETe.

Fig. 4 shows the effect of the Zn and Cd sublimation energies on y. For the given sticking probabilities of the organometallic sources, it is clear from the graph that a small change in the *difference* in the heats of sublimation strongly affects the alloy composition. These changes can be related to the value of K_{sub} in Eq. (33), which increases an order of magnitude for every curve on the graph. A difference of 3.6 kcal/mol is what one calculates from the

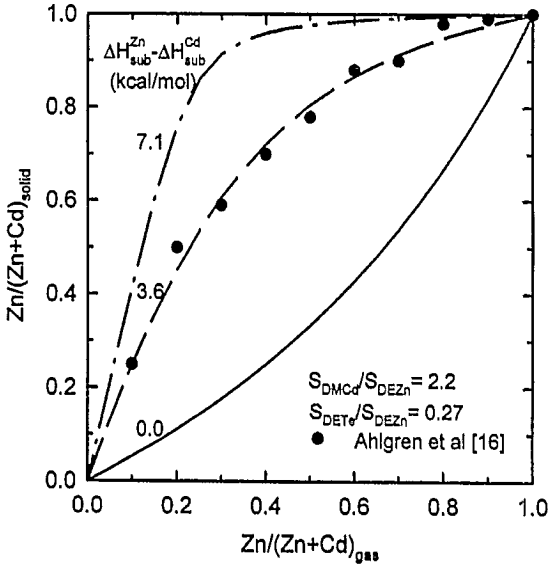

Fig. 4. The effect of varying the difference in the heats of sublimation of Zn and Cd on the solid versus the vapor composition diagram for $Cd_{1-y}Zn_yTe$ OMVPE: (lines) kinetic model, and (●) experimental data.

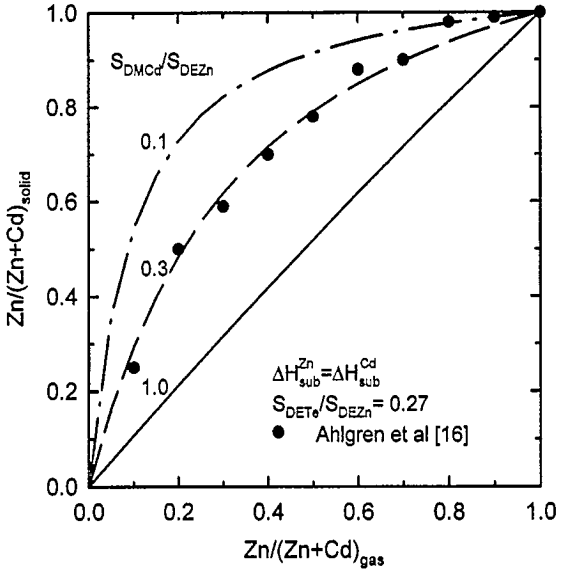

Fig. 5. The effect of varying the ratio of the sticking probability of DMCd over DEZn on the solid versus the vapor composition diagram for $Cd_{1-y}Zn_yTe$ OMVPE: (lines) kinetic model using $\Delta H_{sub}^{Zn} = \Delta H_{sub}^{Cd}$, and (●) experimental data.

heats of sublimation of Zn and Cd reported in the literature [26].

When we assume no discrimination between Zn or Cd sublimation, the alloy composition is exclusively determined by the relative adsorption rates of DEZn and DMCd. This effect is illustrated in Fig. 5. The straight line in the figure for $S_{DMCd}/S_{DEZn} = 1.0$ shows that when the adsorption and desorption rates are the same, there is no segregation between the solid and the gas phase. This result is evident from inspection of Eq. (31). When $K_{sub} = 1$, i.e. $\Delta H_{sub}^{Zn} = \Delta H_{sub}^{Cd}$, this equation simplifies to:

$$y = \frac{K_{DEZn}}{K_{DMCd} + K_{DEZn}} = \frac{1}{A+1}. \qquad (36)$$

Since the molecular weights of DMCd and DEZn are nearly equal, Eq. (36) reduces to $y \approx x$ for $S_{DMCd}/S_{DEZn} = 1.0$. Also note that the sticking probability of DETe is not included in Eq. (36). The relative adsorption rate of the group VI compound only matters when the heats of sublimation of Zn and Cd are significantly different.

It is clear from the above discussion that the extent of zinc segregation depends on the choice of the kinetic parameters. Therefore, it is important to determine their true values. Sublimation energies for Zn and Cd atoms from semiconductor surfaces can be readily obtained by temperature-programmed desorption [34,35]. Sticking probabilities of organometallic compounds on semiconductors have been successfully measured in several laboratories [31,37–39]. Stinespring and Freedman [31] studied the adsorption of DMCd and DMTe on a number of different substrates, including GaAs(100). It was found that at ~ 300 K the initial (reactive) sticking coefficients of DMCd and DMTe on GaAs(100) differed by two orders of magnitude, i.e. 7×10^{-3} and 3×10^{-5}, respectively. Adopting these values for our model and assuming $S_{DMCd}/S_{DEZn} = 1.0$, a good fit to Ahlgren's data is obtained with $\Delta H_{sub}^{Zn} - \Delta H_{sub}^{Cd} = 1.8$ kcal/mol. The energy difference for zinc and cadmium desorption may be this small, and so it is essential that accurate measurements be made. We hope to measure the kinetics of DEZn, DMCd, DMTe and DIPTe decomposition on CdZnTe(111) in the near future.

Lastly, we consider the effects of the OMVPE process variables on the zinc segregation behavior. Shown in Fig. 6 is the dependence of the solid/vapor composition diagram on the VI/II ratio. Using the best-fit parameters from Figs. 2–4, the VI/II ratio is

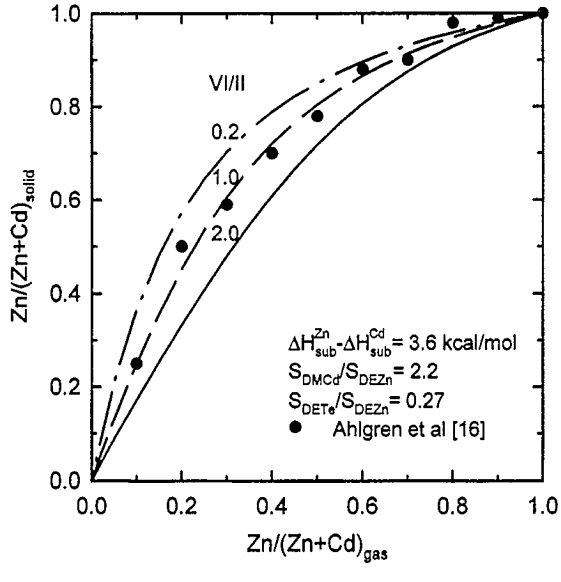

Fig. 6. The effect of varying the VI/II ratio on the solid versus the vapor composition diagram for $Cd_{1-y}Zn_yTe$ OMVPE: (lines) kinetic model, and (●) experimental data.

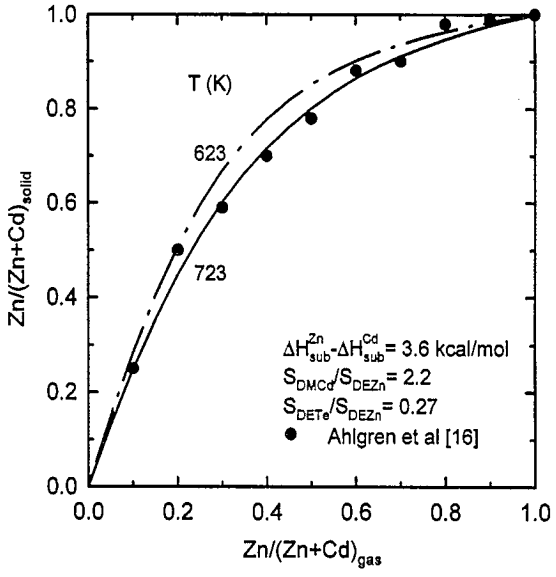

Fig. 7. The effect of varying the substrate temperature on the solid versus the vapor composition diagram for $Cd_{1-y}Zn_yTe$ OMVPE: (lines) kinetic model, and (●) experimental data.

seen to have a small effect on the alloy composition. Nevertheless, zinc segregation is less pronounced at VI/II ratios greater than 2.0. Refering back to Fig. 1, this is the condition where the group II compounds are no longer decomposing in excess of the group VI compound. In other words, sublimation of Zn and Cd is insignificant. This trend suggests that better control of the zinc content in the film may be achieved at high VI/II ratios. However, if the true difference in heats of sublimation is ~ 0.0 instead of 3.6 kcal/mol, then the VI/II ratio will have no effect on the solid/vapor composition diagram.

In Fig. 7, the effect of the substrate temperature on the film composition is presented. The segregation curve is hardly affected by a 100 K change in temperature. This is a result of the small difference in heats of sublimation of Zn and Cd. If this difference is zero ($K_{sub} = 1$), then the curve is completely independent of temperature. Assuming our model is correct, the observation of nonuniform zinc incorporation in the film may be blamed on variations in the partial pressures of DEZn and DMCd above the substrate surface, not on variations in the wafer temperature.

Our model implies that zinc segregation is relatively unaffected by the process variables, but is highly dependent upon the intrinsic reaction kinetics. The heats of sublimation of Zn and Cd and the sticking coefficients of the organometallic precursors play a paramount role in this process. Since the heat of sublimation decreases in the order Zn > Cd ≫ Hg, it may be assumed that segregation always favors the lighter elements. The much lower heat of sublimation of Hg relative to that of Cd explains why such high partial pressures of mercury must be used during HgCdTe OMVPE [23]. Although one has no way to influence the sublimation rates of the group II elements, one might be able to change the relative rates of adsorption of the organometallic precursors. The sticking probability of an organometallic compound partly depends on the strength of its metal–carbon bond. The weaker the metal–carbon bond, the easier the precursor dissociates on the surface and the higher its sticking probability. It is found that the metal–carbon bond strength decreases as the number of carbons bonded to the central carbon atom increases [32]. For example, for most compounds the M–C bond dissociation energy falls in the following order: $CH_3 > C_2H_5 > i\text{-}C_3H_7 > t\text{-}C_4H_9$. Thus, DMZn has a higher bond dissociation energy than DEZn, and it should therefore have a lower sticking probability. Likewise, the sticking probability of DECd should be higher than that of DMCd. This would suggest that the use of DMZn and DECd instead of DEZn and DMCd in CdZnTe OMVPE may diminish the effect of zinc segregation, making it easier to grow films with the desired 4.0% Zn content. Whether or not the OMVPE process can be improved by a more judicious choice of precursors will have to await further experimentation.

6. Conclusions

This study reveals that during CdTe and ZnTe OMVPE, the decomposition of the group II precursors exceeds that of the telluride source, and leads to the sublimation of excess Zn and Cd atoms from the surface. This is similar to what is observed for the OMVPE of III–V compounds, where the group V elements are in excess and sublime off the surface as As_2 and P_2. Our kinetic model shows that the composition of the CdZnTe film is determined by the difference in the heats of sublimation of zinc and

cadmium and by the ratios of the sticking probabilities of DMCd over DEZn and DETe over DEZn. Segregation favors the lighter element with the higher heat of sublimation. However, it maybe possible to counteract this effect by using organometallic precursors that provide a higher sticking probability for the molecule containing the heavier element. The model predicts that except for the partial pressures of the Zn and Cd precursors in the gas, the process conditions have very little impact on the zinc content in the alloy film.

Acknowledgements

We would like to thank the support of the National Science Foundation (grant no. CTS-9121811), G.M. Hughes, and the State of California through the UC MICRO program. Additional funding was provided in the form of a J. William Fulbright Scholarship to M.J.K. and this is also greatly appreciated.

References

[1] R. Dornhauf and G. Nimtz, in: Narrow Gap Semiconductors, Ed. G. Hohler, Tracts in Modern Physics, Vol. 98 (Springer, Berlin, 1983) p. 119.
[2] T. Tung, J. Crystal Growth 86 (1988) 161.
[3] W.E. Tennant, L.J. Kozlowski, L.O. Bubulac, E.R. Gertner and K. Vural, in: IEEE Conf. Ser. 321 (1990) 15.
[4] J.L. Filippozzi, F. Therez, D. Estève, M. Fallahi, D. Kendil, M. da Silva, M. Barbe and G. Cohen-Solal, J. Crystal Growth 101 (1990) 1013.
[5] R.K. Willardson and A.C. Beer, Eds., Semiconductors and Semimetals, Vol. 18 (Academic Press, New York, 1981).
[6] S.M. Johnson, M.H. Kalisher, W.L. Ahlgren, J.B. James and C.A. Cockrum, Appl. Phys. Lett. 56 (1990) 946.
[7] T.J. de Lyon, S.M. Johnson, C.A. Cockrum, O.K. Wu, W.J. Hamilton and G.S. Kamath, J. Electrochem. Soc. 141 (1994) 2888.
[8] A. Kanamori, T. Ota and K. Takahashi, J. Electrochem. Soc. 122 (1975) 1117.
[9] K. Suzuki, K. Inagaki, N. Kimura, I. Tsubono, T. Sawada, K. Imai and S. Seto, Phys. Status Solidi (a) 147 (1995) 203.
[10] S.B. Quadri and J.H. Dinan, Appl. Phys. Lett. 47 (1985) 1066.
[11] R.D. Feldman, R.F. Austin, A.H. Dayem and E.H. Westerwick, Appl. Phys. Lett. 49 (1986) 797.
[12] T.J. de Lyon, J.A. Roth, O.K. Wu, S.M. Johnson and C.A. Cockrum, Appl. Phys. Lett. 63 (1993) 818.
[13] U. Rossner, J. Langier and N. Magnea, J. Crystal Growth 137 (1994) 393.
[14] D. Rajavel and J.J. Zinck, Appl. Phys. Lett. 63 (1993) 322.
[15] T.L. Chu, S.S. Chu, C. Ferekides and J. Britt, J. Appl. Phys. 71 (1992) 5635.
[16] W.L. Ahlgren, S.M. Johnson, E.J. Smith, R.P. Ruth, B.C. Johnston, M.H. Kalisher, C.A. Cockrum, T.W. James, D.L. Arney, C.K. Ziegler and W. Lick, J. Vac. Sci. Technol. A 7 (1989) 331.
[17] G.S. Tompa, T. Salagaj, L. Cook, R.A. Stall, C.R. Nelson, P.L. Anderson, W.H. Wright, W.L. Ahlgren and S.M. Johnson, J. Crystal Growth 107 (1991) 198.
[18] S.M. Johnson, J.A. Vigil, J.B. James, C.A. Cockrum, W.H. Kronkel, M.H. Kalisher, R.F. Risser, T. Tung, W.J. Hamilton, W.L. Ahlgren and J.M. Myrosznyk, J. Electron. Mater. 22 (1993) 835.
[19] I.B. Bhat, N.R. Taskar and S.K. Gandhi, J. Electrochem. Soc. 134 (1987) 195.
[20] B. Liu, A.H. McDaniel and R.F. Hicks, J. Crystal Growth 112 (1991) 192.
[21] W. Bell, J. Stevenson, D.J. Cole-Hamilton and J.E. Hails, Polyhedron 13 (1994) 1253.
[22] M.R. Czerniak and B.C. Easton, J. Crystal Growth 68 (1984) 128.
[23] R.F. Hicks, Proc. IEEE 80 (1992) 1625.
[24] A.H. McDaniel, K.J. Wilkerson and R.F. Hicks, J. Phys. Chem. 99 (1995) 3574.
[25] A.H. McDaniel, B. Liu and R.F. Hicks, J. Crystal Growth 124 (1992) 676.
[26] S.J.C. Irvine and J. Bajaj, J. Crystal Growth 145 (1994) 74.
[27] Y. Nemirovsky, D. Goren and A. Ruzin, J. Electron. Mater. 20 (1991) 609.
[28] R.L. Jackson, Chem. Phys. Lett. 163 (1989) 315.
[29] C.M. Laurie and L.H. Long, Trans. Faraday Soc. 53 (1957) 1431.
[30] S.J.W. Price and A.F. Trotman-Dickenson, Trans. Faraday Soc. 53 (1957) 939.
[31] C.D. Stinespring and A. Freedman, Chem. Phys. Lett. 143 (1988) 584.
[32] G.B. Stringfellow, Organometallic Vapor Phase Epitaxy: Theory and Practice (Academic Press, San Diego, 1989).
[33] R.E. Honig and D.A. Kramer, Vapor Pressure Curves of the Elements, RCA laboratories, Princeton, USA (1968).
[34] M.A. Reuter and J.M. Vohs, Surf. Sci. 262 (1992) 42.
[35] M.A. Reuter and J.M. Vohs, Surf. Sci. 301 (1994) 165.
[36] T.F. Kuech, Mater. Sci. Rep. 2 (1987) 1.
[37] P.E. Gee, H. Qi and R.F. Hicks, Surf. Sci. 330–332 (1995) 135.
[38] J.R. Creighton, Surf. Sci. 234 (1990) 287.
[39] M.L. Yu, U. Memmert, N.I. Buchan and T.F. Kuech, Mater. Res. Soc. Symp. Proc. 204 (1991) 37.